

Sensor Tendons for Soft Robot Shape Estimation

William R. Johnson III, Anjali Agrawala,
Xiaonan Huang, Joran Booth, and Rebecca Kramer-Bottiglio
Dept. of Mechanical Engineering and Materials Science
Yale University, New Haven, CT, USA
will.johnson@yale.edu

Abstract—Tensegrity robots are deformable robots that require highly-stretchable and reliable sensors for proprioception and closed-loop control. We introduce capacitive sensor tendons made of liquid metal electrodes and dielectric silicone that are capable of high strains on the order of hundreds of percent that double as the tensile elements of tensegrity robots. The electromechanical response of the sensor tendons is characterized in ultimate strain, cyclic, and relaxation experiments to demonstrate the sensors' reliability in robotics applications.

Index Terms—tensegrity, shape estimation, capacitive sensing

I. INTRODUCTION

Soft robotics aims to create robots that can survive harsh impacts, adapt to changing environments, and interact safely with humans [1]. Soft sensors are needed to endow soft robots with the proprioception and feedback control necessary to rival their traditional, rigid counterparts [2]. Soft sensors have been developed to sense strain [3], touch [4], texture [5], pressure [6], force [7], temperature [8], and twisting and bending [9]. However, more work is needed to demonstrate the efficacy and reliability of these sensors in robotics.

Tensegrity robots are a class of soft robots made from rigid struts and compliant tendons. High strength-to-weight ratios and the ability to survive harsh impacts make tensegrity robots desirable for autonomous exploration of unpredictable environments including planetary surfaces [10]. However, feedback control and state estimation of tensegrity robots are currently limited by insufficient onboard sensing. [11]. Designing effective and reliable sensors for tensegrity robots is challenging due to their many degrees of freedom and the large deformations they experience. In previous work, researchers have used silicone strain sensors with graphite inclusions [12] and resistive sensors made from conductive thread [13]. However, these sensors were only demonstrated at strains less than 100%, limiting the magnitude of deformations the robot could experience.

Here, we introduce highly stretchable sensor tendons designed for tensegrity robots. The sensor tendons are capacitive strain sensors made from liquid metal paste encapsulated in a silicone elastomer. A common design for tensegrity robots involves a combination of actuated cables and passive cables that act like springs [14]. Accordingly, we designed two types of sensor tendons. *Active tendons* run in parallel to actuated cables. Active tendons need to be reliable sensors for feedback control, but they do not need to exert high forces because the actuators in parallel can do so. *Passive tendons* double as

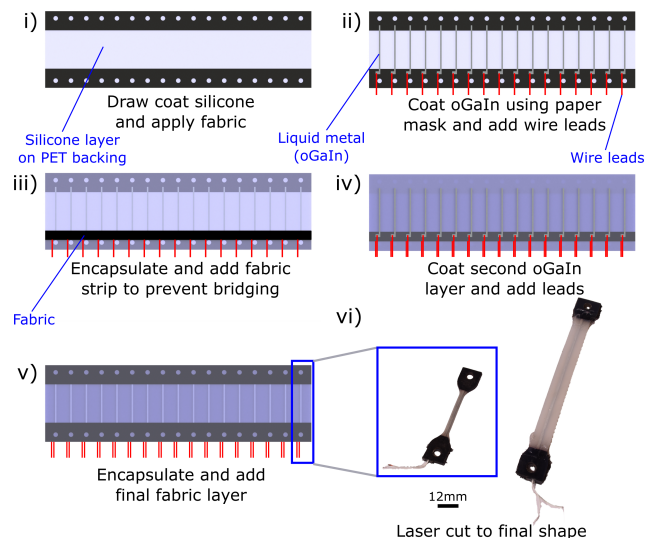


Fig. 1. (i-v) Bulk fabrication process for active tendons using oxidized eutectic gallium-indium (oGaIn). The main differences between fabricating active and passive tendons are the silicone material used and the dimensions of the tendons. (vi) Photograph of the active (left) and passive (right) tendons.

the tensegrity robot's passive springs. Passive tendons have no actuators in parallel, so the forces they exert are essential for the tensegrity robot to recover its original shape after actuation.

For the sensor tendons to be reliable in soft robot applications, they must maintain their electrical and mechanical properties at high strains, through many cycles, and after being held in tension for long time periods. In this work, we demonstrate sensor tendons that meet these standards. In Section II, we describe the design and fabrication process of both active and passive sensor tendons. In Section III, we characterize the sensor tendons' electromechanical response at high strains, in cyclic tests, and in relaxation experiments.

II. DESIGN AND FABRICATION

Sensor tendons are highly stretchable capacitive strain sensors made from silicone elastomers (Eco-Flex 30 or DragonSkin 20; Smooth-On), a liquid metal paste made from eutectic gallium-indium (eGaIn), strain-limiting fabric, and flexible wire leads. Capacitive strain sensors were chosen for their high accuracy, linearity, cyclic stability, and negligible hysteresis [3]. The liquid metal paste is oxidized eGaIn, or

oGaIn, and it is made by stirring eGaIn in ambient air to generate large quantities of amorphous gallium oxide [15], [16]. OGaIn was chosen as the conductive layer for its low electrical resistivity ($2.95 \times 10^{-7} \Omega \text{ m}^{-1}$) and enhanced adhesion to silicone [15]. The sensors are fabricated layer by layer in batches on a backing layer of 0.04" polyethylene terephthalate (PET) and then cut out using a laser cutter. The fabrication process is shown in Figure 1.

Active tendons, which do not need to exert high forces, are made with the relatively soft silicone Eco-Flex 30 while passive tendons, responsible for elastic restoring forces, are made with relatively stiff DragonSkin 20. The fabrication process for both types of sensor tendons is similar. First, a 1 mm layer of silicone is draw coated on a 0.04" sheet of PET. Two strain-limiting fabric strips are impregnated with the silicone and placed on top of the pre-cured layer to form the ends of each sensor. After four hours of curing at room temperature, a paper mask is applied so that a layer of oGaIn can be painted on top with a popsicle stick to form the electrodes. Wire leads are added to 3 mm \times 5 mm pads at the end of each electrode with a drop of oGaIn. A 1 mm layer of silicone with a thin strip of fabric to cover the leads is applied on top. After four hours of curing at room temperature, we apply an extra 1 mm layer of Eco-Flex 30 for the active sensors to prevent bridging between the liquid metal electrodes (this step is not necessary for the passive tendons). After curing, the second layer of oGaIn is applied via a paper mask, and wire leads are added in a similar manner. The last layer is encapsulated in 1 mm of silicone, and a final layer of strain-limiting fabric is applied. After another four hours of curing at room temperature, the batch of sensors is placed in a laser cutter, and the sensors are cut into their final shape. Excess material is removed with a knife. One batch of active tendons produces 17 sensors that are 65 mm in length while one batch of passive tendons produces 14 sensors that are 130 mm in length (lengths are measured from the center of the of the attachment holes on each sensor), although the process could be further scaled. Finally, some silicone adhesive (Sil-Poxy; Smooth-On) is added to either side of the passive sensor tendons to reinforce the stress concentration at the edge of the fabric ends (this step is not necessary for the active tendons).

III. EXPERIMENTAL METHODS

Sensor tendons on tensegrity robots must exhibit electrical and mechanical robustness at high strains, over many cycles, and after long time periods held in tension. Sensor tendons with these properties will enable tensegrity robots to achieve large deformations and reliable closed-loop control. In this section, these properties are demonstrated for active and passive sensor tendons via pulling to failure, cyclic testing, and relaxation experiments.

A. Pull to Failure

Three active tendons and three passive tendons were pulled to failure on a materials testing system (Instron 3345) at a rate of 16 mm/s, and the results are shown in Figure 2. The

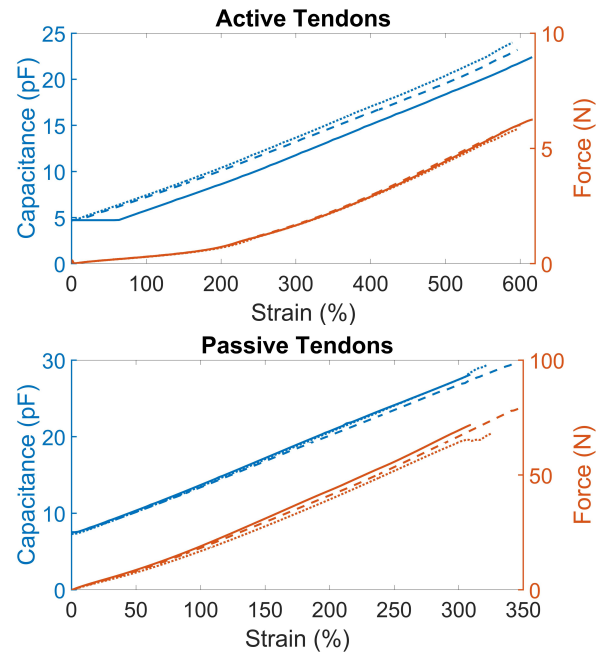


Fig. 2. Three active and passive sensor tendons were pulled to failure. Active tendons broke at 600% strain while passive tendons broke above 300% strain.

active tendons all broke around 600% strain while the passive tendons all broke above 300% strain. The ability to achieve high strains without breaking makes these sensors desirable for tensegrity robots, which experience large deformations during locomotion. The capacitance of each sensor exhibited a linear relationship with strain [17]. Active tendons exerted lower forces than passive tendons because they are thinner and made from a softer material.

B. Cyclic Testing

To remove the Mullins effect [18] before cyclic testing, active and passive sensor tendons were pre-stretched once to the highest strains they would experience during the test, 300% and 140% strain, respectively. During testing, the active and passive tendons were repeatedly extended by 120 mm and 150 mm, respectively, corresponding to the strains they were designed to experience on a tensegrity robot. Three sensors of each type were tested at a rate of 16 mm/s, and the results from one sample of each type are shown in Figure 3. One active tendon broke after 200 cycles, likely due to manufacturing defects, but the rest survived the full 400 cycles of testing. Both active (gauge factor 0.88) and passive (gauge factor 0.86) tendons have stable, repeatable, and linear capacitance values, making them highly reliable sensors for feedback control. The peak force of the active tendons decreases by just 7.5% over 400 cycles. The passive tendons elongate throughout the cyclic testing, leading to a quick reduction in peak force (6.4% over the first 10 cycles) before they begin to stabilize (12.4% decrease over 200 cycles). Unlike the active tendons made from Eco-Flex 30, the passive tendons made from DragonSkin 20 exhibit noticeable mechanical hysteresis.

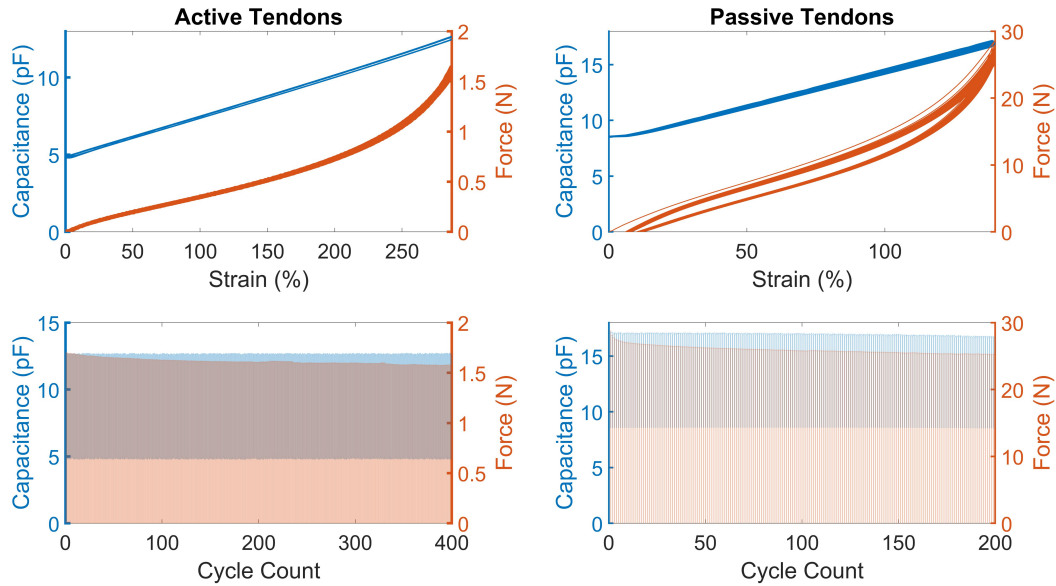


Fig. 3. The cyclic testing results of one active tendon over 400 cycles and one passive tendon over 200 cycles are shown above as a function of engineering strain and below as a function of cycle count. Capacitance is linear and highly repeatable for both sensors. Passive tendons exhibit a 12.4% decrease in force over 200 cycles and notable mechanical hysteresis. The peak force of the active tendons decreases by just 7.5% over 400 cycles.

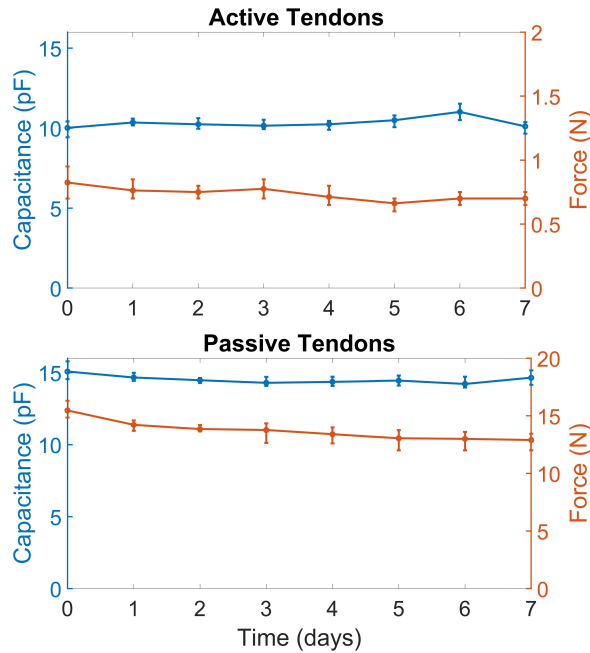


Fig. 4. Active and passive sensor tendons were held in tension at 240% strain and 110% strain, respectively, for seven days. Error bars for the active and passive tendons represent the range of four and three samples, respectively.

C. Relaxation Experiments

Before the relaxation experiments, active tendons were pre-cycled five times to a length of 165 mm (240% strain) and passive tendons five times to a length of 250 mm (110% strain). Then, the sensor tendons were clamped to a 0.25" acrylic frame at the respective 165 mm and 250 mm lengths,

corresponding to the lengths they were designed to have in the resting configuration of a tensegrity robot. The capacitance and force of each sensor was measured once per day for one week, and the results are shown in Figure 4. Of the seven active tendons tested, three broke due to the clamping mechanism; only the sensors that lasted all seven days are shown. None of the three passive tendons tested failed during the week of testing. The capacitance of both types of sensors remained stable after one week as did the force of the active tendons. The slight variations in capacitance measurements may have been the result of re-clamping the sensors at slightly different lengths in between force measurements. On average, the passive tendons show a 1.25 N (8%) decrease in force over the first day before beginning to decrease more gradually (16.6% over seven days).

IV. CONCLUSION

We present the design and facile fabrication of highly stretchable sensor tendons and characterize their effectiveness as sensors for soft robot proprioception. The sensors survive high strains, so they are advantageous for soft robots that experience large deformations. Their electrical response is stable and repeatable after many actuation cycles and long time periods in tension, making them highly reliable sensors for robot state estimation and feedback control. The mechanical stiffness of the passive tendons decreases with cyclic loading or after a few days under constant tension. When used as the restoring springs on tensegrity robots, they will have to be replaced every few days or designed to be stiffer than needed such that they will remain strong enough after their initial relaxation. Future work will demonstrate these sensor tendons estimating the shape of a tensegrity robot in real time.

REFERENCES

- [1] D. Rus and M. T. Tolley, "Design, fabrication and control of soft robots," *Nature*, vol. 521, no. 7553, pp. 467–475, 2015.
- [2] H. Wang, M. Totaro, and L. Beccai, "Toward perceptive soft robots: Progress and challenges," *Advanced Science*, vol. 5, no. 9, p. 1800541, 2018.
- [3] J. Shintake, E. Piskarev, S. H. Jeong, and D. Floreano, "Ultrastretchable strain sensors using carbon black-filled elastomer composites and comparison of capacitive versus resistive sensors," *Advanced Materials Technologies*, vol. 3, no. 3, p. 1700284, 2018.
- [4] C. Larson, B. Peele, S. Li, S. Robinson, M. Totaro, L. Beccai, B. Maz-zolai, and R. Shepherd, "Highly stretchable electroluminescent skin for optical signaling and tactile sensing," *Science*, vol. 351, no. 6277, pp. 1071–1074, 2016.
- [5] D. Hughes and N. Correll, "A soft, amorphous skin that can sense and localize textures," in *2014 IEEE International Conference on Robotics and Automation (ICRA)*. IEEE, 2014, pp. 1844–1851.
- [6] Y.-L. Park, B.-r. Chen, and R. J. Wood, "Soft artificial skin with multi-modal sensing capability using embedded liquid conductors," in *2011 IEEE SENSORS*. IEEE, 2011, pp. 81–84.
- [7] D. M. Vogt, Y.-L. Park, and R. J. Wood, "Design and characterization of a soft multi-axis force sensor using embedded microfluidic channels," *IEEE Sensors Journal*, vol. 13, no. 10, pp. 4056–4064, 2013.
- [8] S. Konishi and A. Hirata, "Flexible temperature sensor integrated with soft pneumatic microactuators for functional microfingers," *Scientific Reports*, vol. 9, no. 1, pp. 1–9, 2019.
- [9] I. Van Meerbeek, C. De Sa, and R. Shepherd, "Soft optoelectronic sensory foams with proprioception," *Science Robotics*, vol. 3, no. 24, p. eaau2489, 2018.
- [10] M. Vespignani, J. M. Friesen, V. SunSpiral, and J. Bruce, "Design of SUPERball v2, a Compliant Tensegrity Robot for Absorbing Large Impacts," in *2018 IEEE/RSJ International Conference on Intelligent Robots and Systems (IROS)*, Oct. 2018, pp. 2865–2871.
- [11] D. S. Shah, J. W. Booth, M. Vespignani, K. Bekris, R. Kramer-Bottiglio *et al.*, "Tensegrity robotics," *Soft Robotics*, vol. 9, no. 4, pp. 639–656, 2022.
- [12] J. W. Booth, O. Cyr-Choiniere, J. C. Case, D. Shah, M. C. Yuen, and R. Kramer-Bottiglio, "Surface actuation and sensing of a tensegrity structure using robotic skins," *Soft Robotics*, vol. 8, no. 5, pp. 531–541, 2021.
- [13] W.-Y. Li, A. Takata, H. Nabae, G. Endo, and K. Suzumori, "Shape recognition of a tensegrity with soft sensor threads and artificial muscles using a recurrent neural network," *IEEE Robotics and Automation Letters*, vol. 6, no. 4, pp. 6228–6234, 2021.
- [14] A. P. Sabelhaus, J. Bruce, K. Caluwaerts, P. Manovi, R. F. Firoozi, S. Dobi, A. M. Agogino, and V. SunSpiral, "System design and locomotion of superball, an untethered tensegrity robot," in *2015 IEEE international conference on robotics and automation (ICRA)*. IEEE, 2015, pp. 2867–2873.
- [15] X. Wang, L. Fan, J. Zhang, X. Sun, H. Chang, B. Yuan, R. Guo, M. Duan, and J. Liu, "Printed conformable liquid metal e-skin-enabled spatiotemporally controlled bioelectromagnetics for wireless multisite tumor therapy," *Advanced Functional Materials*, vol. 29, no. 51, p. 1907063, 2019.
- [16] W. Kong, N. U. H. Shah, T. V. Neumann, M. H. Vong, P. Kotagama, M. D. Dickey, R. Y. Wang, and K. Rykaczewski, "Oxide-mediated mechanisms of gallium foam generation and stabilization during shear mixing in air," *Soft Matter*, vol. 16, no. 25, pp. 5801–5805, 2020.
- [17] W. R. Johnson, J. Booth, and R. Kramer-Bottiglio, "Integrated sensing in robotic skin modules," in *2021 IEEE Sensors*. IEEE, pp. 1–4.
- [18] L. Mullins, "Softening of rubber by deformation," *Rubber chemistry and technology*, vol. 42, no. 1, pp. 339–362, 1969.